Journal of Fluids and Structures 58 (2015) 40–48

Contents lists available at ScienceDirect

Journal of Fluids and Structures

journal homepage: www.elsevier.com/locate/jfs

Modeling and validation of auto-oscillation onset in a constricted tube with application to phonation

Annemie Van Hirtum *, Xavier Pelorson

Gipsa-lab, CNRS UMR 5216, Grenoble University, 11 rue des Mathematiques (BP46), 38402 Grenoble, France

ARTICLE INFO

Article history:
Received 15 December 2014
Accepted 13 July 2015

Keywords:
Physical modeling
Experimental validation
Phonation

ABSTRACT

An experimental study of the auto-oscillation onset is performed for airflow in a rigid tube containing a constriction downstream from a deformable portion as a function of the constriction degree. A quasi-one dimensional laminar flow model in combination with a reduced order mechanical model (symmetric two mass model) provides a physical fluid–structure interaction model of the deformable portion. Mechanical, geometrical and flow model parameters are chosen to match the experimental setup. Modeled as well as experimental results show that a severe constriction ($>80\%$) at first hinders ($\geq 89\%$) and eventually inhibits ($\geq 95\%$) auto-oscillation. Constrictions of different severity occur naturally in voiced speech sound production (phonation) due to articulation. The current study provides quantitative evidence of the role of the vocal tract constriction degree as a control parameter for phonation (voiced speech sound production) since increasing the constriction degree decreases the vocal folds oscillation frequency (decrease by 25%) and increases the minimum pressure needed to initiate oscillation (increase by 80%).

1. Introduction

Normal speech production involves a series of successive transitions between open (*e.g.* neutral vowel or schwa) and obstructed vocal tract configurations (*e.g.* oral occlusive or stop) so that the corresponding area constriction ratio varies between 0 (no constriction) and 1 (total closure).

Since the pioneering work by the late 1960s (Lisker and Abramson, 1964, 1971), a large amount of ongoing literature reports on the crucial role of the vocal tract configuration in laryngeal and articulatory adjustment for voicing and devoicing (see *e.g.* Ohala and Riordan, 1980; Westbury, 1983; Bickley and Stevens, 1986; Lofqvist et al., 1995; Svirsky et al., 1997; Koenig et al., 2008; Pinho et al., 2012). As a result, semi-occlusives are an established tool for voice training and semi-occluded vocal tract exercises are commonly used in speech therapy (see *e.g.* Laukkanen et al., 2008; Cielo et al., 2013).

In contrast to the cited papers on phonetic properties of the phonological voicing contrast, physical and mathematical studies aiming to understand the possible effect of the vocal tract configuration on the vocal folds dynamics are mostly limited to the impact of acoustical coupling for a uniform open vocal tract configuration (Laje et al., 2001; Zhang et al., 2006; Zanartu et al., 2007; Lucero et al., 2012) or to vocal tract acoustics with (Davies et al., 1993) or without (Arnela and Guasch, 2013; Blandin et al., 2015) accounting for convective flow effects. Therefore, the aim of this work is to contribute to the modeling and experimental validation of the impact of a vocal tract constriction on the outcome of a physical phonation

* Corresponding author. Tel.: +33 4 76 57 43 41; fax: +33 4 76 57 47 10.
E-mail address: vanhirtum@granoble-inp.fr (A.V. Hirtum).

http://dx.doi.org/10.1016/j.jfluidstructs.2015.07.004
0889-9746/

model, *i.e.* auto-oscillation of the vocal folds. Such a model approach allows us to express key phonation parameters, such as the pressure threshold at phonation onset, as a function of a limited number of physiologically meaningful parameters to which the vocal tract constriction degree is added. This is a necessary step towards a more extensive study of laryngeal or articulatory adjustment from a physical point of view.

In the following, the impact of a vocal tract by varying constriction degree downstream from a glottal replica (Ruty et al., 2007; Ruty, 2007) on vocal folds auto-oscillation onset is systematically explored using an experimental setup to measure pertinent physical quantities. It was shown (Ruty et al., 2007; Ruty, 2007) that the glottal replica was capable to reproduce phonation pressure thresholds (200–1000 Pa) and auto-oscillation frequencies (100–180 Hz) relevant to the ones observed on human speakers. The streamwise length of a uniformly constricted segment is held constant at 20 mm which corresponds to an order of magnitude of a vocal tract constriction between the tongue and the hard palate (Daniloff et al., 1980; Stevens, 2000). The tube length downstream from the glottal replica has a length of 50 cm which is larger than a human vocal tract (typically 18 cm Daniloff et al., 1980; Stevens, 2000). This is done to avoid secondary noise sources. A simple flow model based on Euler equations is applied to describe the pressure distribution within the vocal tract and to model the influence of the vocal tract constriction on the glottal pressure drop driving phonation. The flow model is then applied to a physical model of speech sound production (van Hirtum et al., 2014) in order to address the impact of a vocal tract constriction from basic fluid dynamical principles for a given vocal tract constriction degree. Acoustical coupling with a downstream pipe representing the supraglottal vocal tract is accounted for in the phonation model. The possible influence of the flow on the wavenumber (Davies et al., 1993) is neglected in the applied model approach as well as the influence of acoustic energy losses along the downstream pipe (Atig et al., 2004; Guilloteau et al., 2014). Moreover, a short upstream pipe is considered in both the model as the experiments. Hence the potential impact of acoustical coupling with an upstream pipe representing the subglottal trachea (Zhang et al., 2006) is not accounted for as well.

2. Method

2.1. Flow model

The onset/offset of vocal fold auto-oscillation is governed by the pressure drop across the glottis. From classical flow studies, it is easily understood that the presence of a constriction in the vocal tract downstream from the glottis alters the pressure distribution within the vocal tract and hence the glottal pressure drop. A simplified vocal tract geometry is schematized in Fig. 1. It consists of a uniform channel with cross-sectional area A_t placed between two constrictions – one at the glottis containing the vocal folds and the other one between the tongue and the hard palate somewhere further downstream with cross sectional area A_{1s}. The total pressure drop ΔP_{tot} yields approximately the imposed subglottal pressure P_{sub}, *i.e.* the pressure immediately upstream from the glottis. The glottal pressure drop ΔP_0 driving vocal folds auto-oscillation is then obtained from the difference of the subglottal pressure P_{sub} and the pressure drop at the constricted vocal tract portion ΔP_1. The pressure drop at the constricted vocal tract portion ΔP_1 is expected to increase as the constriction degree $(1-A_{1s}/A_t)$ increases. Therefore, a pressure recovery immediately downstream from the glottis is expected to occur, which will reduce the pressure drop across the glottis ΔP_0 and hence potentially affects the onset of vocal folds auto-oscillation or phonation.

Based on a non-dimensional analysis of the governing Navier–Stokes equations (Schlichting and Gersten, 2000) and typical values of geometrical and flow characteristics observed for a male adult (Daniloff et al., 1980), the pressure driven flow within the channel is assumed to be laminar (Reynolds number, $\mathrm{Re} \sim O(10^3)$), steady (Strouhal number, $\mathrm{Sr} \ll 1$), incompressible (squared Mach number, $\mathrm{Ma}^2 \ll 0.1$) and two-dimensional (channel aspect ratio or width-to-height ratio, $Ar \gg 4$). The assumption of a two-dimensional flow implies a rectangular glottal cross-section shape for which the height (along the medial–lateral direction) varies along the flow direction $h(x)$ whereas the glottal width (along the anterior–posterior direction) w is fixed. The varying cross-sectional area in the channel can thus be written as $A(x) = h(x) \times w$. Using

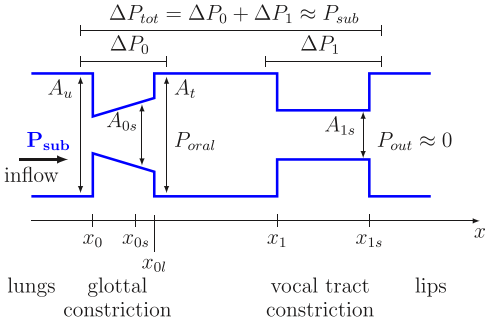

Fig. 1. Schema of glottal and vocal tract geometry enveloping airflow in the streamwise direction (x): pressure $P_{\cdot}$ (subglottal $\cdot = sub$, oral $\cdot = oral$, outlet $\cdot = out$), pressure drop $\Delta P_{\cdot}$ (glottal $\cdot = 0$, oral $\cdot = 1$, total $\cdot = tot$), cross sectional area $A_{\cdot}$ (subglottal $\cdot = u$, glottal flow separation $\cdot = 0s$, downstream end of glottal constriction $\cdot = 0l$, unconstricted vocal tract $\cdot = t$ and uniform vocal tract constriction $\cdot = 1s$).

these assumptions as well as conservation of volume flow rate Q along the streamwise direction x, *i.e.* $dQ/dx=0$, integration of the streamwise momentum equation results in three contributions to the total pressure drop $\Delta P_{tot}=\Delta p_k+\Delta p_v+\Delta p_i$ for the channel geometry depicted in Fig. 1 at time t:

$$\Delta p_k = Q(t)^2\frac{\rho}{2}\left(\frac{1}{A_{0s}(t)^2}+\frac{1}{A_{1s}(t)^2}\right), \tag{1}$$

$$\Delta p_v = -Q(t)12\mu w^2\left(\int_{x_0}^{x_{0s}}\frac{dx}{A(x,t)^3}+\int_{x_1}^{x_{1s}}\frac{dx}{A(x,t)^3}\right), \tag{2}$$

$$\Delta p_i = -\rho\frac{\partial}{\partial t}\left\{Q(t)\left(\int_{x_0}^{x_{0s}}\frac{dx}{A(x,t)}+\int_{x_1}^{x_{1s}}\frac{dx}{A(x,t)}\right)\right\}, \tag{3}$$

with air density $\rho=1.2$ kg/m^3, dynamic viscosity of air $\mu=1.8\times10^{-5}$ Pa s and subscripts as defined in Fig. 1. The first term Δp_k (1) accounts for kinetic pressure losses due to spatial flow acceleration through a channel with varying streamwise area following Euler's equation for an ideal inviscid steady pressure driven flow while assuming $\{A_{0s},A_{1s}\}\ll\{A_u,A_t\}$. The second term Δp_v (2) accounts for viscous pressure losses within constricted channel portions following the lubrication approximation of the Navier–Stokes equations for a flow in a two-dimensional channel. The third term Δp_i (3) accounts for flow inertia following Euler's equation for an ideal inviscid unsteady incompressible pressure driven flow ($dQ/dx=0$). It is seen that for an unconstricted channel the second term at the right-hand sides of Eqs. (1)–(3) can be neglected. The same way (3) vanishes for steady flow.

The outlined flow model is then applied to determine the forces exercised by the flow on a symmetric two-mass vocal folds model outlined in Section 2.2 in order to model the impact of the vocal tract constriction degree $(1-A_{1s}/A_t)$ on vocal folds auto-oscillation onset.

2.2. Symmetric two-mass vocal folds model

The vocal folds ($x_0\le x\le x_{0l}$) mechanics are modeled as a symmetrical low order model in which each vocal fold is represented by two identical masses $m=m_1=m_2$ at positions x_{m_1} and x_{m_2} covered by three massless plates as illustrated in Fig. 2 (Lous et al., 1998; Ruty, 2007; Ruty et al., 2007; van Hirtum et al., 2014). Each of the vocal folds is modeled as a reduced spring–mass–damper system with 2 degrees of freedom driven by the pressure difference $\Delta P_0=P_{sub}-P_{oral}$ across the masses as illustrated in Fig. 2. As in Fig. 1 the subscripts refer to upstream (u), unconstricted vocal tract (t), subglottal (sub) and oral ($oral$). The glottal area $A(x,t)$ is then approximated as a piecewise linear function of x determined by the constant upstream (A_u) and downstream (A_t) channel area and the time-varying areas at the streamwise position of the masses (A_{m_1} and A_{m_2}):

$$A_{i-1,i}(x,t)=\frac{A_i(t)-A_{i-1}(t)}{x_i-x_{i-1}}(x-x_{i-1}), \tag{4}$$

with streamwise position subscripts $i\in\{m_1,m_2,0l\}$ and corresponding $i-1\in\{0,m_1,m_2\}$. The applied models for glottal airflow, vocal folds mechanics and acoustic interaction with a vocal tract downstream from the glottis are severe simplifications of the fluid–structure interaction in the larynx during human sound production.

Following the assumptions outlined in Section 2.1, the anterior–posterior y-dimension is neglected and the time-varying area within the glottis yields $A(x,t)=h(x,t)\times w$ using the assumption of a fixed glottal width w and $x_0\le x\le x_{0l}$. The moving position of flow separation along the diverging portion of the glottis is taken into account using a geometrical criterion $A_{0s}(t)=1.2\times\min(A(x,t))$ defining the position of flow separation x_{0s} in the range $x_{m_1}<x_{0s}\le x_{0l}$ (van Hirtum et al., 2009). At each time instant, the volume flow rate $Q(n+1)$ is determined from the applied subglottal pressure P_{sub} using the flow model outlined in Section 2.1. Using this flow model, the total pressure drop between the channel inlet and outlet ΔP_{tot} yields a quadratic equation of volume flow rate Q. Indeed, from Eqs. (1)–(3), it follows that the contributions to the total

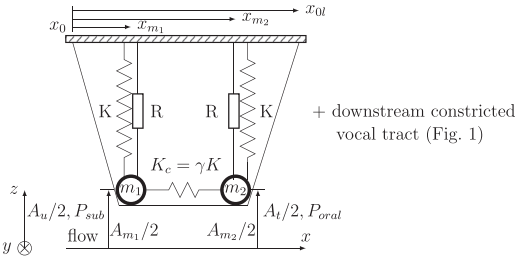

Fig. 2. Schematic representation of a deformable vocal fold modeled as a symmetrical reduced two mass model with $m_1=m_2=m$ (Lous et al., 1998; Ruty, 2007; van Hirtum et al., 2014) constituting the glottal constriction for $x_0\le x\le x_{0l}$ as depicted in Fig. 1.

pressure loss ΔP_{tot} depend either quadratically or linearly on the volume flow rate Q at time step $t=n+1$ since

$$\Delta p_k = \alpha_k Q(n+1)^2 \quad \text{with } \alpha_k = \frac{\rho}{2}\left(\frac{1}{A_{0s}(n)^2}+\frac{1}{A_{1s}(n)^2}\right), \tag{5}$$

$$\Delta p_v = \alpha_v Q(n+1) \quad \text{with } \alpha_v = -12\mu w^2\left(\int_{x_0}^{x_{0s}}\frac{dx}{A(x,n)^3}+\int_{x_1}^{x_{1s}}\frac{dx}{A(x,n)^3}\right), \tag{6}$$

$$\Delta p_i = \alpha_i Q(n+1)+C_i \quad \text{with} \tag{7}$$

$$\alpha_i = -\frac{\rho}{\Delta t}\left(\int_{x_0}^{x_{0s}}\frac{A(x,n-1)}{A(x,n)^2}dx+\int_{x_1}^{x_{1s}}\frac{A(x,n-1)}{A(x,n)^2}dx\right), \tag{8}$$

$$C_i = \frac{\rho Q(n)}{\Delta t}\left(\int_{x_0}^{x_{0s}}\frac{dx}{A(x,n)}+\int_{x_1}^{x_{1s}}\frac{dx}{A(x,n)}\right), \tag{9}$$

where Δt indicates the time increment. Consequently, the following quadratic equation is solved for volume flow rate $Q(n+1)$ using $\Delta P_{tot}\approx P_{sub}$ as illustrated in Fig. 1:

$$\alpha_k Q^2+(\alpha_v+\alpha_i)Q+(C_i-P_{sub})=0. \tag{10}$$

Once the volume flow rate $Q(n+1)$ is estimated, the pressure drops ΔP_0 and ΔP_1 follow directly by combining the first and second right-hand side terms, respectively, of Eqs. (1)–(3). The pressure distribution in the glottis up to flow separation ($x_0\le x\le x_{0s}$) is then obtained as

$$\begin{aligned}P(x,n+1) = P_{sub} &-\frac{\rho}{2}Q(n+1)^2\left(\frac{1}{A(x,n)^2}\right)+12\mu w^2 Q(n+1)\int_{x_0}^{x_{0s}}\frac{dx}{A(x,t)^3}\\ &+\frac{\rho}{\Delta t}Q(n+1)\int_{x_0}^{x_{0s}}\frac{A(x,t-1)}{A(x,t)^2}dx-\frac{\rho}{\Delta t}Q(n)\int_{x_0}^{x_{0s}}\frac{dx}{A(x,t)}.\end{aligned} \tag{11}$$

Downstream from glottal flow separation, the pressure distribution in the glottis for $x_{0s}<x\le x_{0l}$ yields $P(x,n+1)=P_{oral}(n+1)$ with $P_{oral}(n+1)=P(x_{0s},n+1)$. The pressure distribution is then used to determine the forces exercised by the flow on the two-mass vocal folds model.

The acoustic model applied to the vocal tract assumes plane wave propagation so that vocal tract acoustics is represented as a transmission line of N hard-walled sections of fixed length L_k and uniform cross-sectional area $A_k=w\times h_k$ for $k=1,\ldots,N$. In each section the acoustic pressure $p_{ac,k}$ and particle velocity $u_{ac,k}$ are then given as

$$p_{ac,k} = p^+(x-ct)+p^-(x+ct), \tag{12}$$

$$u_{ac,k} = \frac{1}{\rho c}(p^+(x-ct)-p^-(x+ct)), \tag{13}$$

with c denoting the speed of sound in air. Following continuity of acoustic pressure and flow at the junctions between sections k and $k+1$ the reflection coefficient at the junction is $r_k=(A_{k+1}-A_k)/(A_{k+1}+A_k)$ so that for $\Delta t=L_k/c$

$$p^+_{ac,k+1}(n) = \beta_k p^+_{ac,k+1}(n-1)+r_k p^-_{ac,k+1}(n), \tag{14}$$

$$p^-_{ac,k}(n) = -r_k p^+_{ac,k}(n-1)+\phi_k p^-_{ac,k+1}(n), \tag{15}$$

holds propagation constants $\beta_k=1-r_k$ and $\phi_k=1+r_k$. Coupling of the acoustic vocal tract model with the vocal-fold model is assessed by imposing continuity of volume flow and pressure at the glottal exit following the description outlined in Lous et al. (1998) and Ruty (2007):

$$p^+_{ac,oral}(n) = \frac{1}{2}\left(\rho c\frac{Q(n)}{A_1}+P_{oral}(n-1)\right), \tag{16}$$

$$p^-_{ac,oral}(n) = p^-_1(n-1), \tag{17}$$

$$p^+_{ac,1}(n) = p^+_{ac,oral}(n-1), \tag{18}$$

$$p^-_{ac,1}(n) = r_1 p^+_1(n)+\phi_1 p^-_1(n-1), \tag{19}$$

with $p_{ac,oral}(n)=p^+_{ac,oral}(n)+p^-_{ac,oral}(n)$ being the acoustic pressure at the glottis. The pressure difference at the glottis then becomes $\Delta P_0=P_{sub}-P_{oral}-p_{ac,oral}$. The acoustic model is completed by considering a low frequency approximation of the impedance of a radiating piston (Ruty, 2007).

The symmetrical mechanical model shown in Fig. 2 describes the movement of the two masses perpendicular to the flow along the z direction (Lous et al., 1998; Ruty, 2007; Ruty et al., 2007; van Hirtum et al., 2014). As before, a rectangular glottal

area with fixed width w is assumed. The mechanical model parameters are mass m, spring stiffness K, damping R and coupling spring stiffness between the two masses $K_c=\gamma K$ with $\gamma=0.5$. Mass m, stiffness K and damping R are defined as the value per unit width. In addition, a critical glottal area threshold $A_{crit}=0.5$ mm^2 is used to trigger vocal folds collision when $A_{min}<A_{crit}$ with minimum glottal area $A_{min}=\min(A_{m_1},A_{m_2})$. Whenever collision is detected, the values of K and R are increased to $K_{crit}=4K$ and $R_{crit}=R+2\sqrt{K_{crit}m}$, respectively. The two masses have the same mechanical parameters K, R and m. With these notations the mechanical model is written as two coupled equations (Lous et al., 1998; Ruty, 2007; Ruty et al., 2007; van Hirtum et al., 2014):

$$m\frac{d^2A_{m_1}}{dt^2}+R\frac{dA_{m_1}}{dt}+K(1+\gamma)A_{m_1}-\gamma KA_{m_2}=F_1(A_{m_1},A_{m_2},\Delta P_0), \tag{20}$$

$$m\frac{d^2A_{m_2}}{dt^2}+R\frac{dA_{m_2}}{dt}+K(1+\gamma)A_{m_2}-\gamma KA_{m_1}=F_2(A_{m_1},A_{m_2},\Delta P_0), \tag{21}$$

with initial areas in the absence of flow $A^0_{m_1}$ and $A^0_{m_2}$ and $F_1=w\int_{x_0}^{(x_{m_2}-x_{m_1})/2}\lambda(x)p(x)\,dx$, $F_2=w\int_{(x_{m_2}-x_{m_1})/2}^{x_{0l}}\lambda(x)p(x)\,dx$ expressing the forces exerted by the fluid on the masses along the z-axis on the first and second mass, respectively where $0\le\lambda(x)\le1$ since only part of the pressure exerted by the fluid is taken into account in the forces. From Eqs. (20) and (21), it is seen that – when neglecting damping – stability or instability resulting in auto-oscillation onset depends on the balance between stabilizing stiffness K and pressure force related to the pressure difference ΔP_0 (Ruty et al., 2007; van Hirtum et al., 2014).

Finite difference discretization is applied to Eqs. (20) and (21) (Lous et al., 1998; Ruty, 2007):

$$\frac{A_{m_1}(n+1)+A_{m_1}(n-1)-2A_{m_1}(n)}{\Delta t^2}+\frac{R}{m}\frac{A_{m_1}(n+1)-A_{m_1}(n)}{\Delta t}+\frac{K(1+\gamma)}{m}A_{m_1}-\frac{\gamma K}{m}A_{m_2}=\frac{1}{m}F_1(A_{m_1},A_{m_2},\Delta P_0), \tag{22}$$

$$\frac{A_{m_2}(n+1)+A_{m_2}(n-1)-2A_{m_2}(n)}{\Delta t^2}+\frac{R}{m}\frac{A_{m_2}(n+1)-A_{m_2}(n)}{\Delta t}+\frac{K(1+\gamma)}{m}A_{m_2}-\frac{\gamma K}{m}A_{m_1}=\frac{1}{m}F_2(A_{m_1},A_{m_2},\Delta P_0), \tag{23}$$

which expresses $A_{m_1}(n+1)$ and $A_{m_2}(n+1)$ as a function of their values at previous time steps n and $n-1$, mechanical model parameters (m,K,R,γ) and the z-components of the forces exerted by the fluid flow F_1 an F_2. Concretely, the pressure forces are computed as detailed in Lous et al. (1998) and Ruty (2007).

2.3. Experimental setup

In order to experimentally assess the impact of a vocal tract constriction on auto-oscillation onset, experiments are performed using a mechanical replica enveloping two constrictions as depicted in Fig. 3. Air is supplied by a compressor (Copco GA7). The compressor is connected to a pressure reservoir of 0.75 m^3 ('lung' replica). Pressure can be provided from a few Pa up to 4000 Pa by means of a pressure regulator (Norgren type 11-818-987) and manual valve situated upstream from the pressure reservoir. A mechanical glottal replica is mounted to the reservoir to which a downstream channel (vocal tract replica) is attached. The mechanical glottal replica (width $w=25$ mm) contains two latex tubes filled with water representing two vocal folds (Ruty et al., 2007). Mechanical properties of the vocal folds can be modified by changing the water pressure P_{water} inside the latex tubes from 3000 Pa up to 6000 Pa by means of a water column. A uniform channel of length $L=50$ cm, height 25 mm and width 25 mm is attached to the glottal replica. The height h_c of a rectangular uniform constriction at the channel end (length 20 mm and constant width $w=25$ mm) was changed either steadily or following a prescribed motor-driven motion at 0.4 Hz. Besides the unconstricted case ($h_c=h_t$), height h_c was varied (and then held steady) from 0.8 mm up to 4.1 mm, corresponding to 3% up to 16% of the uniform downstream pipe area so that the constriction degree $(1-h_c/h_t)$ ranges from 84% to 97% (Table 1). Note that for a rectangular constriction with constant width the vocal tract constriction degree $1-A_{1s}/A_t$, which is the main variable in the flow model (1)–(3), reduces to $1-h_c/h_t$. Therefore, in the following the constriction degree is denoted $1-h_c/h_t$ since it is an explicit function of the experimentally varied variable h_c. The pressure immediately upstream from the glottal replica P_{sub} and the pressure immediately upstream

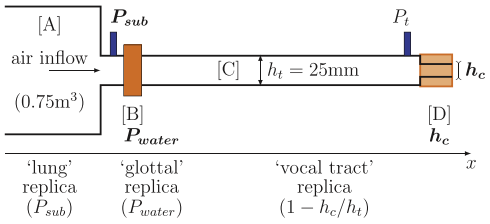

Fig. 3. Schematic overview of experimental setup: 'lungs' (upstream pressure P_{sub}) [A], 'glottal' replica (internal water pressure P_{water}) (Ruty et al., 2007) [B], unconstricted 'vocal tract' channel with constant width $w=25$ mm and constant height $h_t=25$ mm (vocal tract pressure P_t) [C] and uniform constriction with constant width $w=25$ mm and variable height $h_c\le h_t$ (due to the constant width the area constriction degree becomes $1-h_c/h_t$). h_c can either be maintained constant or a forced movement can be applied using a motor [D].

from the constricted portion P_t are measured by pressure sensors (Kulite, XCS-0.93-0.35-Bar-G) positioned in the pressure taps indicated in Fig. 3. The volume flow rate is not measured since the main model parameter is the upstream pressure P_{sub} from which the volume flow rate is estimated as expressed in (10) and the oscillation is driven by the pressure difference across the vocal folds replica following (21).

From Fig. 4, it is seen that for an unconstricted channel ($1-h_c/h_t=0\%$) the required upstream pressure to sustain auto-oscillation, corresponding to the phonation threshold pressure, is minimal ($P_{sub,0\%}=313$ Pa) for $P_{water}\approx 5100$ Pa and the corresponding oscillation frequency yields $f_{osc,0\%}=176$ Hz. Results reported in the next section are all obtained for $P_{water}=5100$ Pa and corresponding mechanical model parameters (initial aperture area, stiffness and damping for $P_{water}\approx 5100$ Pa) of the glottal replica are taken from Ruty et al. (2007) where these values are derived experimentally for the same glottal replica using the same setup.

3. Results and discussion

Fig. 5 illustrates vocal tract pressure P_t normalized by mean upstream pressure $P_{sub,mean}$ observed using the experimental setup depicted in Fig. 3 while varying constriction degree $1-h_c/h_t$ sinusoidally (motor-driven constriction at 0.4 Hz) between 93% and 99.8%. Auto-oscillation of the vocal folds replica is observed when the constriction degree decreases while auto-oscillation ceases when the constriction degree increases. In addition, the simulated pressure P_t estimated using the symmetric two-mass vocal folds model (van Hirtum et al., 2014) with the flow model outlined in Section 2.1 is plotted as well. Modeled data provide a qualitative approximation of the experimental observations including the observed tendency of oscillation onset and offset as a function of constriction degree. Consequently, the experimental setup as well as the model is capable to reproduce 'voicing–devoicing' sequences solely by varying the constriction degree within the vocal tract since all other control parameters are held constant during both experiment ($P_{sub,mean}$ and P_{water}) and simulation ($P_{sub,mean}$, stiffness, damping, initial aperture area).

The impact of a constriction on auto-oscillation behavior of the glottal replica is systematically studied for static vocal tract configurations with constant constriction degree $1-h_c/h_t$ while the upstream pressure P_{sub} is gradually increased in the same way (to a maximum value $P_{sub,max}\approx 545$ Pa). Measured pressure values (P_{sub} and P_t) for constriction degrees 89% ($h_c=2.7$ mm) and 95% ($h_c=1.2$ mm) are illustrated in Fig. 6 as a function of time and frequency. For a constriction

Table 1
Overview of experimentally assessed static vocal tract constriction heights (h_c) and associated constriction degrees ($1-h_c/h_t$).

h_c (mm)	25[a]	4.1	2.7	2.4	1.9	1.6	1.2	0.8
$1-h_c/h_t$ (%)	0[a]	84	89	90	92	94	95	97

[a] Unconstricted channel, *i.e.* $h_c=h_t$ in Fig. 3.

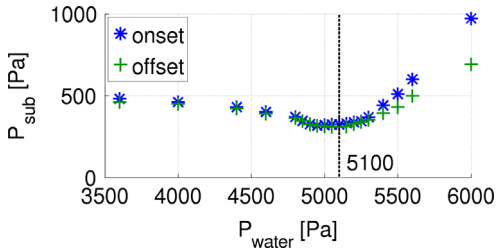

Fig. 4. Measured upstream pressures P_{sub} at auto-oscillation onset (∗) and offset (+) for an unconstricted channel ($h_c=h_t$) as a function of vocal folds internal water pressure P_{water}. A minimum pressure $P_{sub,0\%}=313$ Pa is observed for $P_{water}\approx 5100$ Pa (dashed vertical line).

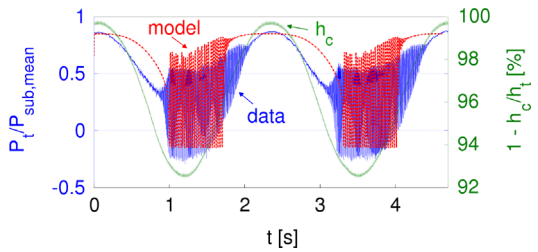

Fig. 5. Illustration of measured (data) and modeled (model) vocal tract pressure P_t normalized by the mean value of the upstream pressure $P_{sub,mean}$ (left axis) for a sinusoidally (motor-driven constriction at 0.4 Hz) varied constriction degree $1-h_c/h_t$ (right axis) as a function of time t.

degree of 89%, the pressure signal P_t (Fig. 6a) starts to oscillate (onset) around its mean value of 0 Pa as the upstream pressure P_{sub} is increased and oscillation stops (offset) as the upstream pressure is decreased. For a constriction degree of 95% no oscillation is observed and the mean value of P_t is proportional to the upstream pressure P_{sub} indicating that the pressure drop $P_{sub}-P_t$ is reduced compared to the case of 89% and is therefore no longer sufficient to sustain auto-oscillation which supports the flow model expressed in Section 2.1.

Fig. 7 shows measured auto-oscillation onset and offset pressures P_{sub} and associated auto-oscillation frequencies f_{osc} normalized by their values observed in the absence of a constriction ($P_{sub,0\%}$ and $f_{osc,0\%}$) as a function of constriction degree $1-h_c/h_t$ (Table 1). The upstream pressure P_{sub} (Fig. 7a) needed to sustain auto-oscillation onset and offset increases from values observed in the absence of a constriction ($1-h_c/h_t \leq 90\%$) to almost twice this value ($1-h_c/h_t \approx 94\%$) until auto-oscillation is no longer observed ($1-h_c/h_t \geq 95\%$). The measured oscillation frequency f_{osc} (Fig. 7b) decreases with 10% up to 25% as the constriction degree $1-h_c/h_t$ increases until no auto-oscillation is observed. Consequently, the presence of a

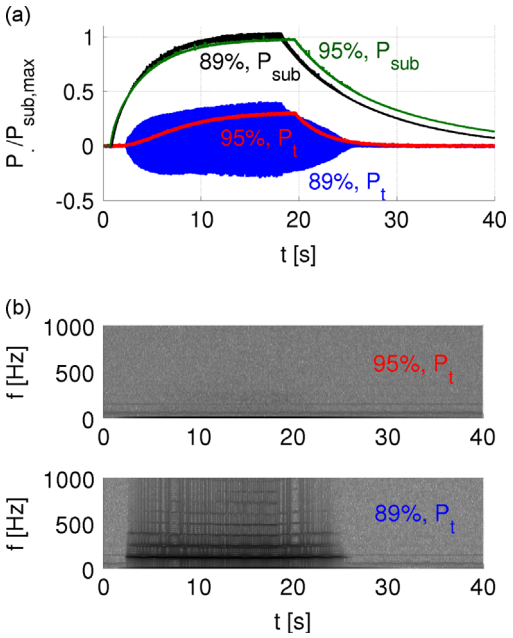

Fig. 6. Illustration of time–frequency properties of measured pressure signals for two constriction degrees $1-h_c/h_t = 89\%$ ($h_c = 2.7$ mm) and $1-h_c/h_t = 95\%$ ($h_c = 1.2$ mm): (a) P_{sub} and P_t normalized by $P_{sub,max} \approx 545$ Pa as a function of time t, and (b) spectrogram of P_t.

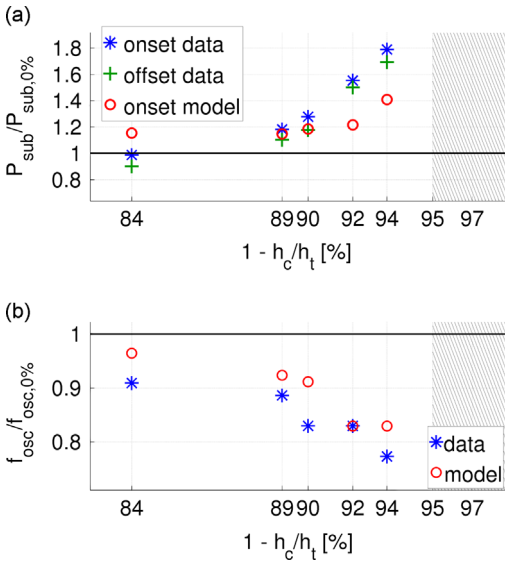

Fig. 7. Influence of constriction degree $(1-h_c/h_t)$ on auto-oscillation features: (a) normalized onset pressure P_{sub}, (b) normalized auto-oscillation frequency f_{osc}. No auto-oscillation is observed in the shaded area. Ratio 1 (horizontal line) corresponds to no constriction (subscript 0%).

constriction affects the measured minimum upstream pressure needed to sustain auto-oscillation and to a less extent it affects the associated oscillation frequency.

Modeled values of upstream pressure P_{sub} and oscillation frequency f_{osc} at oscillation onset are indicated in Fig. 7 as a function of constriction degree $(1-h_c/h_t)$ as well. Modeled and measured values agree qualitatively and exhibit the same tendency: increase of onset pressure P_{sub} associated with a decrease of oscillation frequency f_{osc} as the constriction degree $(1-h_c/h_t)$ increases until no oscillation is observed for constriction degrees $\geq 95\%$. Quantitative agreement between measured and predicted onset pressures P_{sub} (Fig. 7a) is within $<20\%$ for constriction degrees $(1-h_c/h_t)$ up to 90%. For larger constriction degrees ($>90\%$), modeled values underestimate the onset pressure with 40% indicating that additional losses occur which are not accounted for in the flow model. The error in the predicted oscillation frequencies f_{osc} (Fig. 7b) is independent of constriction degree $(1-h_c/h_t)$ since modeled values systematically overestimate measured oscillation frequencies ($\leq 10\%$).

Experimental and modeled data provide evidence that a severe constriction (degree $>80\%$) in the tube downstream from the glottal replica affects phonation features since at oscillation onset the required pressure P_{sub} as well as the associated oscillation frequency f_{osc} are influenced. Consequently, current data show that the constriction degree is a phonation control parameter since all other control parameters are held constant. Experimentally two major control parameters are related to the glottal replica: the internal water pressure P_{water} (determining the stiffness applied in the two-mass model describing the vocal folds mechanics) and the initial glottal aperture height (and hence glottal area). Increasing those glottal control parameters will increase the oscillation frequency f_{osc} of a glottal replica (Ruty et al., 2007; Cisonni et al., 2011) whereas increasing the constriction degree has the opposite effect. Consequently, the combination of different control parameters might contribute to the understanding of different control strategies for phonation onset parameters P_{sub} and f_{osc} observed on human speakers, such as laryngeal adjustment affecting the initial glottal area (Bickley and Stevens, 1986; Lofqvist et al., 1995; Koenig et al., 2008; Pinho et al., 2012) or oral cavity enlargement reducing the glottal pressure drop (Lisker and Abramson, 1964, 1971; Ohala and Riordan, 1980; Westbury, 1983; Svirsky et al., 1997). In addition, taking vocal tract parameters (such as the constriction degree) into account when modeling phonation might in the long run lead to the understanding of a universal (cross-language and cross-speaker observed phenomena) intrinsic fundamental frequency, *i.e.* a lower intrinsic fundamental frequency (up to 25 Hz) for low vowels (such as /a/) compared to high vowels (such as /i/) (Crandall, 1925; Whalen and Levitt, 1995). Note that 25 Hz corresponds to variation of f_{osc} (10%) observed when using the experimental setup to vary the constriction degree. Nevertheless, no conclusion can be formulated based solely on the current study since besides the constriction degree also the streamwise location of the constriction varies during vowel production. In addition, the effect of viscosity in constricted channel portions is modeled (2) relying on the assumption of two-dimensional flow. This assumption is motivated for the assessed experimental replica and supported by observations of the glottal aperture during normal phonation of human speakers (Svec et al., 2000). However, the cross section shape of constricted portions due to articulation is highly variable (Daniloff et al., 1980) and the assumption of two-dimensional flow for the vocal tract constriction is therefore only a first approximation. In order to improve the model outcome for human articulation, the viscous term (2) related to viscous losses within the vocal tract constriction can be adapted to account for the cross section shape of the vocal tract constriction as proposed in (van Hirtum et al., 2014) without changing the model approach.

4. Conclusion

Experimental and modeled data show that increasing the constriction degree ($>80\%$) results in an increase of the minimum upstream pressure required to sustain oscillation (with 80%) and a decrease of the associated oscillation frequency (with 25%) until oscillation stops for constriction degrees greater than 95%. Predicted and measured oscillation frequencies match within 10% for all assessed constriction degrees. Predicted and measured upstream pressure values at oscillation onset match to within 20% for constriction degrees $<90\%$ and the accuracy decreases (discrepancy between 20% and 40%) for constriction degrees $>90\%$. Therefore, the constriction degree downstream of a deformable section in a rigid tube is an important parameter affecting auto-oscillation of the deformable portion. The current study quantifies the impact of a single constriction on the oscillation threshold pressure and associated oscillation frequency and identifies a range of constriction degrees for which the effect is major (constriction degrees $>80\%$). Moreover, the applied model approach is capable to capture the impact of the constriction degree. Therefore, the applied model approach can be used in future studies to investigate the mechanisms underlying the onset of instability leading to auto-oscillation. When applied to phonation, the current study provides strong evidence that the constriction degree of the vocal tract needs to be taken into account in physical models of phonation and might in term contribute to the understanding of phenomena such as intrinsic fundamental frequency and the role of laryngeal or articulatory adjustment strategies for phonation.

The tube length in the current experiments was set to 50 cm. It is of interest to expand current findings to shorter tube lengths as well as to differ the streamwise position of the constricted tube segment. Moreover, it is of interest to vary geometrical features of the constriction such as its shape and its length.

Acknowledgements

This work was partly supported by EU-FET Grant (EUNISON 308874).

References

Arnela, M., Guasch, O., 2013. Finite element computation of elliptical vocal tract impedances using the two-microphone transfer function method. Journal of the Acoustical Society of America 133, 4197–4209.
Atig, M., Dalmont, J., Gilbert, J., 2004. Saturation mechanism in clarinet-like instruments, the effect of the localised non-linear losses. Applied Acoustics 65, 1133–1154.
Bickley, C., Stevens, K., 1986. Effects of a vocal tract constriction on the glottal source: experimental and modelling studies. Journal of Phonetics 14, 373–382.
Blandin, R., Arnela, M., Laboissière, R., Pelorson, X., Guasch, O., van Hirtum, A., Laval, X., 2015. Effects of higher order propagation modes in vocal tract like geometries. Journal of the Acoustical Society of America 137, 832–843.
Cielo, C., de Moraes Lima, J., Christmann, M., Brum, R., 2013. Semioccluded vocal tract exercises: literature review. Revista CEFAC 15 (6), 1679–1689.
Cisonni, J., van Hirtum, A., Pelorson, X., Lucero, J., 2011. The influence of geometrical and mechanical input parameters on theoretical models of phonation. Acta Acustica 97, 291–302.
Crandall, J., 1925. The sounds of speech. Bell System Technical Journal 4 (4), 586–626.
Danilof, R., Schuckers, G., Feth, L., 1980. The Physiology of Speech and Hearing, Prentice-Hall, Englewood Cliffs, NJ, p. 453.
Davies, P., McGowan, R., Shadle, C., 1993. Practical flow duct acoustics applied to the vocal tract. In: Vocal Fold Physiology: Frontiers in Basic Science. Singular Publishing Co., San Diego, pp. 93–142.
Guilloteau, A., Guillemain, P., Kergomard, J., 2014. Dependence of the acoustic power produced by a woodwind on the tonehole size. In: Proceedings of ISMA, Le Mans, France, pp. 1–5.
Koenig, L., Lucero, J., Mencl, W., 2008. Distinctive features and laryngeal control. Journal of Voice 22 (6), 709–720.
Laje, R., Gardner, T., Mindlin, G., 2001. Continuous model for vocal fold oscillations to study the effect of feedback. Physical Review E 64, 1–7.
Laukkanen, A., Titze, I., Hoffman, H., Finnegan, E., 2008. Effects of a semioccluded vocal tract on laryngeal muscle activity and glottal adduction in a single female subject. Folia Phoniatrica et Logopaedica 60, 298–311.
Lisker, L., Abramson, A., 1964. A cross-language study of voicing in initial stops: acoustical measurements. Word 20, 384–422.
Lisker, L., Abramson, A., 1971. Distinctive features and laryngeal control. Language 47, 767–785.
Lofqvist, A., Koenig, L., McGowan, R., 1995. Vocal tract aerodynamics in /aca/ utterances: measurements. Speech Communication 16, 49–66.
Lous, N., Hofmans, G., Veldhuis, N., Hirschberg, A., 1998. A symmetrical two-mass vocal-fold model coupled to vocal tract and trachea, with application to prosthesis design. Acta Acoustica 84, 1135–1150.
Lucero, J., Lourenco, K., Hermant, N., van Hirtum, A., Pelorson, X., 2012. Effect of source-tract acoustical coupling on the oscillation onset of the vocal folds. Journal of the Acoustical Society of America 132, 403–411.
Ohala, J., Riordan, C., 1980. Passive Vocal Tract Enlargement During Voiced Stops. Report of the Phonology Laboratory 5, University of Berkeley, USA, pp. 78–88.
Pinho, C., Jesus, L., Barney, A., 2012. Weak voicing in fricative production. Journal of Phonetics 40 (5), 625–638.
Ruty, N., 2007. Modèles d'interactions fluide parois dans le conduit vocal. Applications aux voix et aux pathologies (Ph.D. thesis). Institut National Polytechnique de Grenoble, Grenoble, France.
Ruty, N., Pelorson, X., van Hirtum, A., Lopez, I., Hirschberg, A., 2007. An in-vitro setup to test the relevance and the accuracy of low-order models of the vocal folds. Journal of the Acoustical Society of America 121, 479–490.
Schlichting, H., Gersten, K., 2000. Boundary Layer Theory. Springer Verlag, Berlin, 2000, p. 801.
Stevens, K., 2000. Acousic Phonetics. MIT Press, MA, USA, p. 607.
Svec, J., Horacek, J., Sram, F., Vesely, J., 2000. Resonance properties of the vocal folds: in vivo laryngoscopic investigation of the externally excited laryngeal vibrations. Journal of the Acoustical Society of America 108 (4), 1397–1406.
Svirsky, M., Stevens, K., Matthies, M., Manzella, J., Perkell, J., Wilhelms-Tricarico, R., 1997. Tongue surface displacement during bilabial stops. Journal of the Acoustical Society of America 102, 562–571.
van Hirtum, A., Cisonni, J., Pelorson, X., 2009. On quasi-steady laminar flow separation in the upper airways. Communications in Numerical Methods in Engineering 25, 447–461.
van Hirtum, A., Wu, B., Pelorson, X., Lucero, J., 2014. Influence of glottal cross-section shape on phonation onset. Journal of the Acoustical Society of America 136, 853–858.
Westbury, J., 1983. Enlargement of the supraglottal cavity and its relation to consonant voicing. Journal of the Acoustical Society of America 73, 1322–1336.
Whalen, D., Levitt, A., 1995. The universality of intrinsic F_0 of vowels. Journal of Phonetics 23, 349–366.
Zanartu, M., Mongeau, L., Wodicka, G., 2007. Influence of acoustic loading on an effective single mass model of the vocal folds. Journal of the Acoustical Society of America 120, 1558–1569.
Zhang, Z., Neubauer, J., Berry, D., 2006. The influence of subglottal acoustics on laboratory models of phonation. Journal of the Acoustical Society of America 120, 1558–1569.